Missing Texture Reconstruction Method Based on Error Reduction Algorithm Using Fourier Transform Magnitude Estimation Scheme

Takahiro Ogawa, *Member, IEEE* and Miki Haseyama, *Senior Member, IEEE*,

***Abstract*—A missing texture reconstruction method based on an error reduction (ER) algorithm including a novel estimation scheme of Fourier transform magnitudes is presented in this correspondence. In our method, Fourier transform magnitude is estimated for a target patch including missing areas, and the missing intensities are estimated by retrieving its phase based on the ER algorithm. Specifically, by monitoring errors converged in the ER algorithm, known patches whose Fourier transform magnitudes are similar to that of the target patch are selected from the target image. In the second approach, the Fourier transform magnitude of the target patch is estimated from those of the selected known patches and their corresponding errors. Consequently, by using the ER algorithm, we can estimate both the Fourier transform magnitudes and phases to reconstruct the missing areas.**

***Index Terms*—Image reconstruction, texture analysis, Fourier transform magnitude estimation, phase retrieval, error reduction algorithm.**

I. Introduction

Restoration of missing areas in digital images has been intensively studied due to its many useful applications such as removal of unnecessary objects and error concealment. Therefore, many methods for realizing these applications have been proposed. Generally, the methods previously reported in the literature are broadly classified into two categories, structure-based reconstruction [1] and texture-based reconstruction [2]. In this correspondence, we focus on the texture-based reconstruction approach and limit our target to reconstruction of gray scale images.

Most algorithms, which focus on texture reconstruction, estimate missing areas by using statistical features of known textures within the target image as training patterns. Specifically, they approximate patches within the target image in lower-dimensional subspaces and derive the inverse projection for the corruption to estimate missing intensities. In this scheme, several multivariate analyses such as PCA [3], [4] and sparse representation [5] have been used for obtaining low-dimensional subspaces. In addition to the above reconstruction schemes, many texture synthesis-based reconstruction methods have been proposed. Efros et al. first proposed a pioneered method [2], and their ideas were improved by many researchers [6]–[9]. A good survey of those methods has been shown by Fidaner [10].

It should be noted that conventional methods generally calculate texture feature vectors whose elements are raster scanned intensities in clipped patches. However, when the patches are clipped in intervals different from the periods of the textures, the obtained feature vectors become quite different from each other even if they are the same kinds of textures. This is always caused by the mismatch between clipping interval and periods of textures. Thus, it becomes difficult to generate subspaces that can correctly approximate the clipped patches in low dimensions or find best-matched examples. Then the reconstruction ability of missing textures also becomes worse.

T. Ogawa is with Graduate School of Information Science and Technology, Hokkaido University, Sapporo, 060-0814 JAPAN E-mail:ogawa@lmd.ist.hokudai.ac.jp

M. Haseyama is with Graduate School of Information Science and Technology, Hokkaido University, Sapporo, 060-0814 JAPAN E-mail:miki@ist.hokudai.ac.jp

This work was partly supported by Grant-in-Aid for Scientific Research (B) 21300030, Japan Society for the Promotion of Science (JSPS).

In order to solve the above problem, we propose a missing texture reconstruction method based on an error reduction (ER) algorithm [11] using a new Fourier transform magnitude estimation scheme. Given a known Fourier transform magnitude of a target image, the ER algorithm retrieves its phase from an image domain constraint to estimate its unknown intensities. In our method, we focus on a unique characteristic of Fourier transform magnitudes, shift invariant characteristic. The Fourier transform magnitudes of patches clipped from the same kinds of textures become similar to each other. Therefore, Fourier transform magnitudes can be effectively utilized as texture features, and the mismatch between clipping interval and periods of textures can also be represented by the phases. In order to reconstruct missing textures, the proposed method introduces the following two novel approaches into the ER algorithm. First, our method enables selection of similar[1] known patches, which are optimal for the reconstruction of target patches including missing areas, based on errors converged by the ER algorithm. Next, from the selected known patches and their corresponding errors, the proposed method performs the estimation of the Fourier transform magnitudes of target patches. Then, from the estimated Fourier transform magnitudes, we retrieve their phases based on the ER algorithm and enable successful reconstruction of missing areas.

II. Characteristic of Textures

In this section, we describe the characteristic of texture images to show the effectiveness of the use of Fourier transform magnitudes as texture features. In the reconstruction of texture images, Fourier transform magnitudes have important roles for representing their features. We show an interesting example for confirming the characteristic of textures in Fig. 1. This figure shows two patches that are clipped from the same texture image and a patch clipped from a different texture image. When we calculate distances of intensity values between patches, not only different kinds of textures but also the same kinds of textures have large distances. Therefore, in the conventional methods that directly utilize intensities within patches, it becomes difficult to accurately represent the features of those textures. On the other hand, the distances of the Fourier transform magnitudes can reflect the visual differences of textures as shown in Fig. 1. Since similar patterns periodically appear within texture images, it seems that texture features of clipped patches can be represented by Fourier transform magnitudes and the gap between the clipping interval and the period of textures can be absorbed by the phases, i.e., the Fourier transform magnitude can be utilized as the shift invariant features of textures. From this point, we should utilize Fourier transform magnitudes as the features of textures instead of the use of directly obtained intensities.

III. Texture Reconstruction Method Based on The ER Algorithm

In this section, we present the texture reconstruction method based on the ER algorithm. The ER algorithm [11], which is one of the iterative Fourier transform algorithm and is widely used for phase retrieval, enables reconstruction of a target image by iteratively applying both Fourier and image constraints. In the proposed method, a patch f ($w \times h$ pixels) including missing areas is clipped from the target image, and its missing textures are estimated from the other known areas. For the following explanations, we denote two areas whose intensities are unknown and known within the target patch f as Ω and $\bar{\Omega}$, respectively. Furthermore, the proposed method utilizes known patches f^i ($i = 1, 2, \cdots, N$) that are clipped from

[1]In the following explanations, similar patches mean ones whose textures are similar.

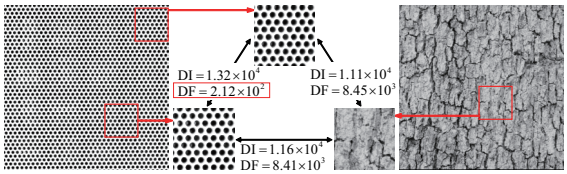

Fig. 1. Example for confirming the characteristic of textures. It should be noted that DI and DF respectively represent the mean differences of intensity values and Fourier transform magnitudes.

the target image in the same interval, where N is the number of clipped patches. Note that we simply clip training patches in a raster scanning order from the upper-left of the target image. In the proposed method, we first estimate the Fourier transform magnitude of the target patch f based on converged errors in the ER algorithm (See III-A). Next, reconstruction of the target patch f is realized by using the ER algorithm from the estimated Fourier transform magnitude (See III-B).

A. Estimation of Fourier Transform Magnitude

In this subsection, we explain the algorithm for estimating the Fourier transform magnitude of the target patch f. In order to estimate the Fourier transform magnitude, we first select patches whose Fourier transform magnitudes are similar to that of f from f^i ($i = 1, 2, \cdots, N$) and calculate the distances of the Fourier transform magnitudes between the target patch f and the selected patches. Unfortunately, the true distances of the Fourier transform magnitudes cannot be directly calculated for the target patch f since it contains the missing area Ω. Therefore, the proposed method utilizes the errors converged in the ER algorithm under the following two constraints as new criteria e^i ($i = 1, 2, \cdots, N$).

Fourier Constraint:
The Fourier transform magnitude of f is the same as that of f^i, $|F^i(u,v)|$ ($u = 1, 2, \cdots, w$, $h = 1, 2, \cdots, h$).
Image Constraint:
Since the intensities in the area $\bar{\Omega}$ of the target patch f are known, these values are fixed.

Then the error converged after T_1 iterations in the ER algorithm is calculated as follows:

$$e^i = \sum_{u=1}^{w}\sum_{v=1}^{h}\left(\left|F_{T_1}(u,v)\right| - \left|F^i(u,v)\right|\right)^2, \tag{1}$$

where $\left|F_{T_1}(u,v)\right|$ represents the Fourier transform magnitude of the target patch f obtained after T_1 iterations.

As shown in [11], the ER algorithm is one of the steepest descend algorithms that minimize the errors of Fourier transform magnitudes under the image domain constraint. Therefore, we can regard the error e^i ($i = 1, 2, \cdots, N$) converged in the ER algorithm as the minimum distance[2] of the Fourier transform magnitude between the two patches f and f^i. Then M patches whose criteria e^i are smaller than those of other known patches are selected. For the following explanation, the selected patches and their calculated distances e^i are respectively denoted as $\hat{f}^j$ and $\hat{e}^j$ ($j = 1, 2, \cdots, M$).

From the above procedures, we can select M known patches $\hat{f}^j$ similar to f in terms of Fourier transform magnitudes and their minimum distances $\hat{e}^j$. By using the known Fourier transform magnitudes $|\hat{F}^j(u,v)|$ of $\hat{f}^j$ and their corresponding distances $\hat{e}^j$ ($j = 1, 2, \cdots, M$), the proposed method estimates the Fourier transform magnitude of the target patch f based on the idea of MDS [12]. First, we define a vector $\boldsymbol{\xi}^j$ whose elements are the raster scanned values of each Fourier transform magnitude $|\hat{F}^j(u,v)|$. Similarly, the vector of the Fourier transform magnitude of the target patch f is denoted as $\boldsymbol{\xi}$. From the matrix $\boldsymbol{\Xi}$ ($= [\boldsymbol{\xi}^1, \boldsymbol{\xi}^2, \cdots, \boldsymbol{\xi}^M]$), we can obtain the following singular value decomposition:

$$\begin{aligned}\boldsymbol{\Xi}\mathbf{H} &= \mathbf{U}\boldsymbol{\Lambda}\mathbf{V}^\top \\ &= \mathbf{U}\mathbf{Z}.\end{aligned} \tag{2}$$

In the above equation, $\boldsymbol{\Lambda}$ is a $q \times q$ singular value matrix, where q is the rank of $\boldsymbol{\Xi}$, and $\mathbf{U}$ and $\mathbf{V}$ are $wh \times q$ and $M \times q$ orthonormal matrices, respectively. Vector/matrix transpose is represented by the superscript $^\top$. The matrix $\mathbf{Z} = [\mathbf{z}^1, \mathbf{z}^2, \cdots, \mathbf{z}^M]$ satisfies $\mathbf{Z} = \boldsymbol{\Lambda}\mathbf{V}^\top$. Furthermore, $\mathbf{H} = \mathbf{I} - \frac{1}{M}\mathbf{1}\mathbf{1}^\top$ is an $M \times M$ centering matrix, where $\mathbf{I}$ is the identity matrix and $\mathbf{1} = [1, 1, \cdots, 1]^\top$ is an $M \times 1$ vector. Following [12],

$$-2\mathbf{Z}^\top\mathbf{z} = \left(\mathbf{e}^2 - \mathbf{e}_0^2\right) - \frac{1}{M}\mathbf{1}\mathbf{1}^\top\left(\mathbf{e}^2 - \mathbf{e}_0^2\right) \tag{3}$$

is satisfied. The vector $\mathbf{z}$ in the above equation is

$$\mathbf{z} = \mathbf{U}^\top\left(\boldsymbol{\xi} - \bar{\boldsymbol{\xi}}\right), \tag{4}$$

where $\bar{\boldsymbol{\xi}} = \frac{1}{M}\sum_{j=1}^{M}\boldsymbol{\xi}^j$. Furthermore, $\mathbf{e}^2$ is an $M \times 1$ vector whose j-th element corresponds to $\hat{e}^j$, and $\mathbf{e}_0^2 = [\|\mathbf{z}^1\|^2, \|\mathbf{z}^2\|^2, \cdots, \|\mathbf{z}^M\|^2]^\top$. Then the estimation result $\hat{\boldsymbol{\xi}}$ of $\boldsymbol{\xi}$ is realized by the following procedures. First,

$$\begin{aligned}\hat{\mathbf{z}} &= -\frac{1}{2}\left(\mathbf{Z}\mathbf{Z}^\top\right)^{-1}\mathbf{Z}\left(\mathbf{e}^2 - \mathbf{e}_0^2\right) \\ &= -\frac{1}{2}\boldsymbol{\Lambda}^{-1}\mathbf{V}^\top\left(\mathbf{e}^2 - \mathbf{e}_0^2\right).\end{aligned} \tag{5}$$

Therefore, from Eq. (5), the estimation result $\hat{\boldsymbol{\xi}}$ is obtained as follows:

$$\hat{\boldsymbol{\xi}} = \mathbf{U}\hat{\mathbf{z}} + \bar{\boldsymbol{\xi}}. \tag{6}$$

By using the above equation, we can finally obtain the estimation result $|\hat{F}(u,v)|$ of the Fourier transform magnitude for the target patch f.

B. Texture Reconstruction Algorithm

The algorithm for texture reconstruction of the missing area Ω within the target patch f by using the estimated Fourier transform magnitude $|\hat{F}(u,v)|$ is presented in this subsection. Based on the ER algorithm under the following two constraints, the proposed method recovers the phase of f to reconstruct the missing texture in Ω.

Fourier Constraint:
The Fourier transform magnitude of the target patch f is $|\hat{F}(u,v)|$.
Image Constraint:
Since the intensities in the area $\bar{\Omega}$ of the target patch f are known, these values are fixed.

By applying the above two constraints to the target patch f in T_2 times, we try to retrieve its phase. Note that the estimated Fourier transform magnitude $|\hat{F}(u,v)|$ generally contains errors, so that f tends not to satisfy the Fourier constraint. In such a case, the reconstruction results within Ω may be degraded due to these errors. Therefore, the proposed method simply introduces an alternative procedure that renews $|\hat{F}(u,v)|$ utilized as the Fourier constraint into the ER algorithm. Specifically, the renewal of the Fourier transform magnitude used as the Fourier constraint is performed after every $T_3 (T_3 < T_2)$ iterations as follows:

$$|\hat{F}_{m+1}(u,v)| = |\hat{F}_m(u,v)| + \beta\left\{|F_m(u,v)| - |\hat{F}_m(u,v)|\right\}, \tag{7}$$

[2]It should be noted that the Fourier constraint utilized in the ER algorithm is non-convex. Thus, it is difficult to perfectly obtain the global optimal solution by this algorithm.

where m represents mth iteration in the ER algorithm, and $|\hat{F}_m(u,v)|$ is the Fourier transform magnitude used as the Fourier constraint in mth iteration. Note that the initial values of $|\hat{F}_0(u,v)|$ become those of $|\hat{F}(u,v)|$ in our method. Furthermore, $|F_m(u,v)|$ represents the Fourier transform magnitude of the target patch f in mth iteration. The value β is a positive constant. In the above equation, $|\hat{F}_m(u,v)|$ is renewed in such a way that the distance from the Fourier transform magnitude $|F_m(u,v)|$ of the target patch satisfying the image constraint is minimized. Then, by iterating this modified ER algorithm, phase retrieval satisfying the above two constraints can be realized. Therefore, we can reconstruct the missing area Ω within the target patch f. Finally, the proposed method clips patches including missing areas and performs their reconstruction to estimate all missing intensities in the target image. It should be noted that in order to realize this scheme, we have to determine the order in which patches along the fill-front of missing areas are filled. We call this order "patch priority". In the proposed method, the patch priorities are determined by the method proposed by Criminisi et al. [7].

As shown in the above algorithm, the proposed method can retrieve the phase of the target patch f to reconstruct the missing area Ω. As shown in the previous subsection, we can estimate the Fourier transform magnitude, and the rest unknown component is only its phase. Therefore, the phase must be retrieved from the obtained Fourier transform magnitude under the constraint of the known intensities within $\bar{\Omega}$. As described above, it is well known that the ER algorithm is one of the steepest descend algorithms which minimize the mean square error between the known Fourier transform magnitude and that of the target patch. Furthermore, if we assume that the Fourier transform magnitude of the target patch f can be perfectly estimated by the previous subsection, the ER algorithm is the best one to estimate its phase. Therefore, in this subsection, we adopt the ER algorithm-based scheme for retrieving the phase of the target patch f to reconstruct the missing area Ω.

IV. Experimental Results

In this section, we verify the performance of the proposed method from results of experiments in order to confirm its effectiveness. First, we prepared test images including missing areas and performed their reconstruction by using the proposed method and several conventional methods. One reconstruction example is shown in Fig. 2. In this figure, we show results of the proposed method and the conventional methods in [7], [3], [4], [8], [9]. Since these conventional methods are benchmarking and state-of-the-art methods which directly use intensity values within patches, they are suitable for comparison with our method using Fourier transform magnitudes as texture features. In addition, reconstruction results by a method which selects the known patches used for the reconstruction of the target patch based on the distances of known intensities within $\bar{\Omega}$ are shown in Fig. 2(d). This is shown to justify the use of the Fourier transform magnitudes as textures features and the use of the converged errors in the ER algorithm as the similarity measurements of textures in the proposed method.

In this experiment, we simply determined the parameters of the proposed method as follows: $M = 5$, $T_1 = 50$, $T_2 = 200$, $T_3 = 20$, and $\beta = 0.1$. Furthermore, the patch size was fixed to 31×31 or 15×15 pixels, i.e., we used square patches of size 31×31 or 15×15 pixels, where Fig. 2 shows results of the patch size 31×31 pixels. In this experiment, we simply set the patch size in such a way that the chessboard distances between pixels within the patch and the centered pixel become equal to or less than 15 or 7 pixels. Note that when we use the patch of size 15×15 pixels, the number of training examples is about 16 times larger than that when using the patch of size 31×31 pixels. It should be noted that many more training examples and much smaller patches were generally used in studies on conventional methods employed in this experiment, and accurate performance could be achieved. In Fig. 3, we show reconstruction examples obtained by our method and the conventional methods [7], [8], [9]. These results are obtained by using patches of size 15×15 pixels. Then not only the proposed method but also the conventional methods [7], [8], [9] can improve the performance compared to the results shown in Fig. 2. If the number of training examples becomes smaller and patch size becomes larger, the representation performance of textures becomes worse. This means that the conditions for reconstruction become worse. In this experiment, we used such difficult conditions in order to make the difference in the performances of the proposed method and conventional methods clearer. As shown in Fig. 2, it can be seen that the use of the proposed method achieved improvements compared to the conventional methods. Furthermore, by comparing Figs. 2(c) and (d), we can see the ER algorithm-based proposed approach using Fourier transform magnitudes as texture features is effective for the accurate missing texture reconstruction.

Next, for other test images shown in Fig. 4, we performed the same experiments. In this figure, the results of reconstruction by the proposed method and the conventional methods are also shown[3]. Results of quantitative evaluation using the MSE and the SSIM index are shown in Tables I and II. The SSIM index is one of the most representative quality measures widely used in the field of image processing, and it is alternative to the MSE [13]. It has also been reported that the SSIM index is a better quality measure than the MSE and its variants. Note that the conventional methods in [3] and [4] simply perform the reconstruction of patches including missing areas in a raster scanning order. Then, for some test images, since target patches of size 15×15 pixels contain missing areas in the whole parts, their methods cannot reconstruct those missing areas. Thus, in Tables I and II, we only show the results of the patch size 15×15 pixels by our method and the conventional methods in [7], [8] and [9] that can adaptively determine the reconstruction order, i.e., the patch priority. From the obtained results, some improvements by the proposed method can be confirmed.

As shown in the previous section, the proposed method utilizes the Fourier transform magnitudes of patches as texture features. They have a unique characteristic, i.e., a shift-invariant characteristic, and features of textures can be represented by using fewer examples than those in the case of conventional methods. Furthermore, the proposed method estimates unknown Fourier transform magnitudes of target patches from similar known patches based on the use of errors converged in the ER algorithm. Then, from the estimated Fourier transform magnitude, their phases are also retrieved by the ER algorithm. This means that the proposed method can perform the reconstruction of missing textures by effectively using those texture features.

Finally, we discuss the limitation of the proposed method. As show in Section I, we limit the target of the proposed method to the reconstruction of gray scale texture images. Therefore, it is difficult to accurately restore structural components by only using Fourier transform magnitudes representing texture features. Some examples are shown in Figs. 5 and 6. If the target missing edges have simple structures, the proposed method tends to reconstruct them successfuly. However, if the size of missing areas becomes larger and the edge structures also become more complex, it is difficult for our method to accurately recover them even if the filling order is determined by [7] which can consider the structure components. When structural

[3]Due to the limitation of pages, we simply select one conventional method for each test image.

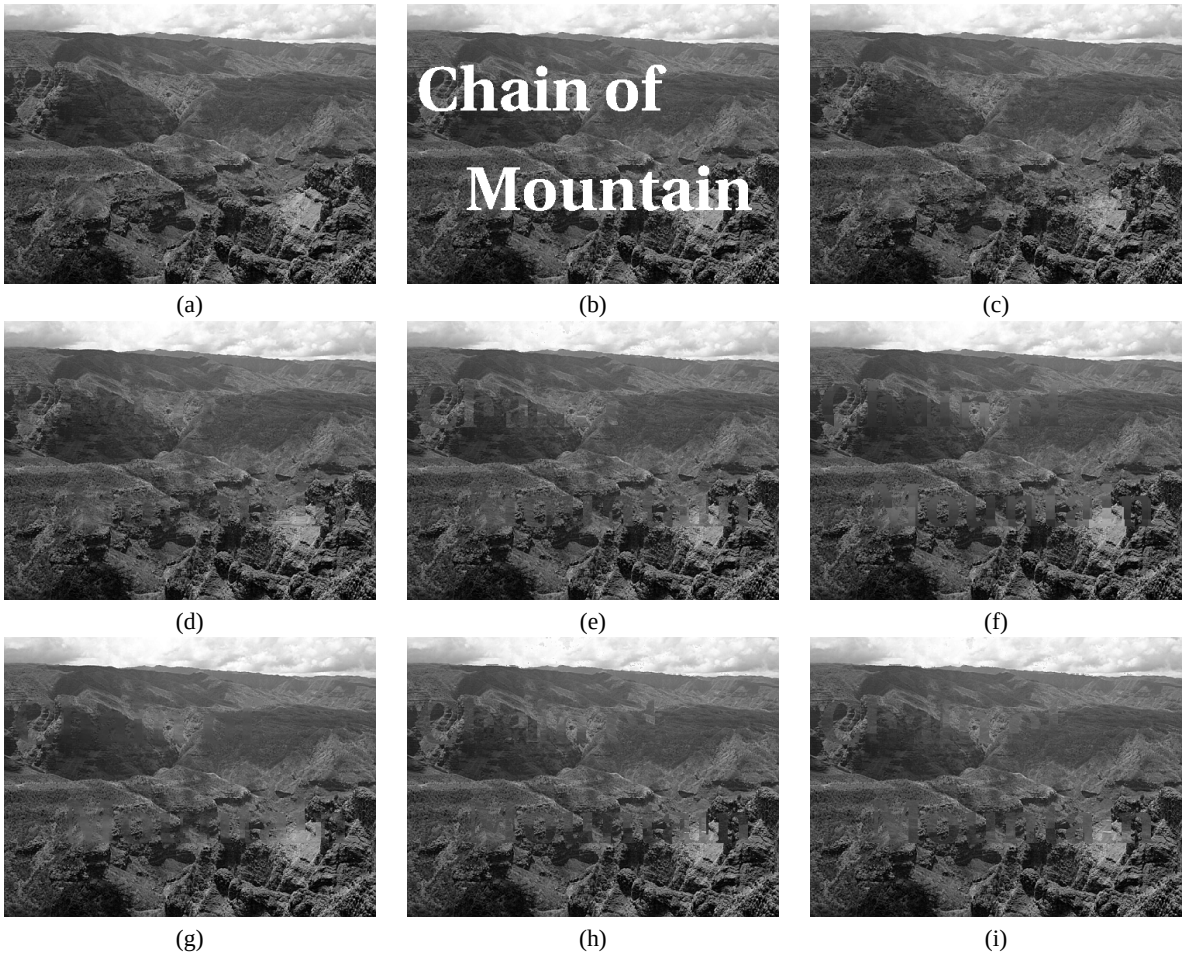

Fig. 2. (a) Original image (480×360 pixels, 8-bit gray levels), (b) Corrupted image including text regions (8.9% loss), (c) Reconstructed image obtained by the proposed method, (d) Reconstructed image by the scheme that the known patches used for the reconstruction of the target patch are selected based on the distances of known intensities within Ω, (e) Reconstructed image obtained by the conventional method in [7], (f) Reconstructed image obtained by the conventional method in [3], (g) Reconstructed image obtained by the conventional method in [4], (h) Reconstructed image obtained by the conventional method in [8], (i) Reconstructed image obtained by the conventional method in [9]. (Patch size: 31×31 pixels, 106 training patches)

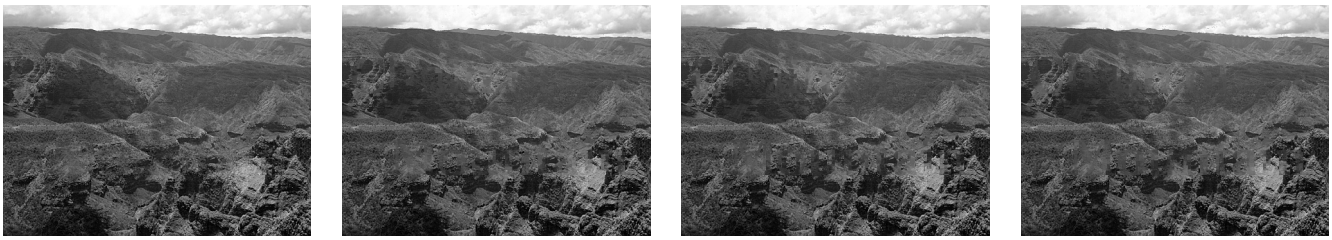

Fig. 3. Reconstruction results of Fig. 2(b) obtained in the following conditions: the patch size is 15×15 pixels, and the number of training examples is about 16 times larger than that of Fig. 2: (a) Reconstructed image obtained by the proposed method, (b) Reconstructed image obtained by the conventional method [7], (c) Reconstructed image obtained by the conventional method [8], (d) Reconstructed image obtained by the conventional method [9].

components in target images are reconstructed, color information becomes very important. It should be noted that if the proposed method is directly applied to color images, reconstruction results might suffer from some spurious colors since we do not consider the relationship between different color components. Therefore, in order to solve this problem, we have to introduce a new scheme for avoiding spurious colors into the proposed method. Since this is one of the biggest issues to accurately reconstruct structural components, we will have to study this point in our future work. Next, we discuss the computation cost of the proposed method. When using the same patch size, the computation times of our method are about 1.5–3.0 times slower than those of the conventional method [7][4]. Note that in [14], Kwok et al. realized about 15–50 times faster reconstruction than that of the method in [7]. The proposed method includes some procedures that require high computation costs such as the exhaustive search for best-matched known patches for each target patch including missing areas. Thus, by introducing some alternative approaches included in some conventional methods [14] into the searching procedures of our method, improvement in the speed of the computation can be expected. This topic will be investigated in the subsequent studies.

[4]The experiments were performed on a personal computer using Intel(R) Core(TM) i7 950 CPU 3.06 GHz with 8.0 Ggytes RAM. The implementation was performed by using Matlab.

Fig. 4. (a)–(d) Original images ((a) 480×359 pixels, (b) 640×480 pixels, (c) 480×640 pixels, (d) 640×480 pixels), (e)–(h) Corrupted images of (a)–(d) ((e) 8.9% loss, (f) 5.4% loss, (g) 6.2% loss, (h) 6.7% loss), (i)–(l) Reconstruction results of (e)–(h) by the proposed method, (m)–(p) Reconstruction results by the conventional methods ((m) Reference [3], (n) Reference [7], (o) Reference [8], (p) Reference [9]). All of these images are 8-bit gray levels. In order to save the pages, we show the rotated images for (c), (g), (k) and (o). Furthermore, the numbers of training patches were respectively 107, 215, 209 and 218 in (e)–(h), and the patch size was set to 31×31 pixels.

Fig. 5. Reconstruction example 1 obtained by applying the proposed method to larger size missing areas: (a) Target image (480×362 pixels, 8-bit gray levels), (b) Reconstructed image obtained by the proposed method. (Patch size: 15×15 pixels)

Fig. 6. Reconstruction example 2 obtained by applying the proposed method to larger size missing areas: (a) Target image (818×546 pixels, 8-bit gray levels), (b) Reconstructed image obtained by the proposed method. (Patch size: 15×15 pixels)

V. Conclusions

A new missing texture reconstruction method based on the ER algorithm including a Fourier transform magnitude estimation scheme is presented in this correspondence. The proposed method utilizes Fourier transform magnitudes as texture features and enables missing texture reconstruction by retrieving their phases based on the ER algorithm. In this algorithm, we newly introduce the Fourier transform magnitude estimation approach by the errors converged in the ER algorithm. This approach realizes accurate texture feature estimation and enables successful reconstruction of the missing areas. Consequently, some improvements of the proposed method over the previously reported methods are confirmed.

TABLE I
PERFORMANCE COMPARISON (MSE) OF THE PROPOSED METHOD AND THE CONVENTIONAL METHODS.

Test image	Reference [7]	Reference [3]	Reference [4]	Reference [8]	Reference [9]	Our method
Fig. 2(a) (31×31 pixels)	27.80	23.50	**18.23**	32.03	27.01	31.78
Fig. 4(a) (31×31 pixels)	68.00	**38.14**	38.22	68.37	55.92	50.16
Fig. 4(b) (31×31 pixels)	31.23	29.15	**26.56**	37.84	32.21	42.22
Fig. 4(c) (31×31 pixels)	58.29	43.57	**38.47**	64.86	51.51	52.90
Fig. 4(d) (31×31 pixels)	46.34	30.66	**24.94**	54.84	37.69	37.92
Average (31×31 pixels)	46.33	33.00	**29.28**	51.89	40.87	43.00
Fig. 2(a) (15×15 pixels)	24.38	-	-	30.20	**22.97**	23.67
Fig. 4(a) (15×15 pixels)	56.62	-	-	64.00	50.26	**36.78**
Fig. 4(b) (15×15 pixels)	**32.41**	-	-	37.22	32.79	33.87
Fig. 4(c) (15×15 pixels)	59.85	-	-	62.90	52.94	**37.88**
Fig. 4(d) (15×15 pixels)	36.68	-	-	43.56	35.73	**23.90**
Average (15×15 pixels)	41.99	-	-	47.58	38.94	**31.22**

TABLE II
PERFORMANCE COMPARISON (SSIM) OF THE PROPOSED METHOD AND THE CONVENTIONAL METHODS.

Test image	Reference [7]	Reference [3]	Reference [4]	Reference [8]	Reference [9]	Our method
Fig. 2(a) (31×31 pixels)	0.9393	0.9315	0.9398	0.9371	0.9420	**0.9542**
Fig. 4(a) (31×31 pixels)	0.9219	0.9330	0.9351	0.9255	0.9292	**0.9422**
Fig. 4(b) (31×31 pixels)	**0.9634**	0.9585	0.9614	0.9605	0.9626	0.9631
Fig. 4(c) (31×31 pixels)	0.9470	0.9492	0.9532	0.9451	0.9495	**0.9576**
Fig. 4(d) (31×31 pixels)	0.9458	0.9501	0.9535	0.9425	0.9511	**0.9587**
Average (31×31 pixels)	0.9435	0.9445	0.9486	0.9421	0.9469	**0.9552**
Fig. 2(a) (15×15 pixels)	0.9459	-	-	0.9411	0.9489	**0.9634**
Fig. 4(a) (15×15 pixels)	0.9274	-	-	0.9282	0.9334	**0.9556**
Fig. 4(b) (15×15 pixels)	0.9640	-	-	0.9617	0.9631	**0.9693**
Fig. 4(c) (15×15 pixels)	0.9517	-	-	0.9465	0.9513	**0.9671**
Fig. 4(d) (15×15 pixels)	0.9535	-	-	0.9498	0.9538	**0.9715**
Average (15×15 pixels)	0.9485	-	-	0.9455	0.9501	**0.9654**

In future work, we have to adopt a new scheme in order to realize successful structure reconstruction. Some researchers have reported simultaneous reconstruction approaches of structural and texture parts that enable selection of a suitable reconstruction method for each area [15], [16], [17]. This means they can adaptively select the two reconstruction methods which respectively perform accurate structure and texture restoration. Thus, this scheme may provide one solution to the above problem. We also have to realize an improved method which can reconstruct color images successfully. Furthermore, the reduction of the computation costs in the proposed method should also be realized. We need to complement the above points in subsequent studies.

REFERENCES

[1] C. Ballester, M. Bertalmio, V. Caselles, G. Sapiro, "Filling-In by Joint Interpolation of Vector Fields and Gray Levels," *IEEE Trans. on Image Processing*, pp.1200–1211, vol.10, no.8, 2001.

[2] A. A. Efros and T. K. Leung, "Texture synthesis by nonparametric sampling," *IEEE International Conference on Computer Vision*, Corfu, Greece, pp.1033–1038, Sept. 1999.

[3] T. Amano and Y. Sato, "Image interpolation using BPLP method on the eigenspace," *Systems and Computers in Japan*, vol.38, no.1, pp.87-96, Jan. 2007.

[4] T. Ogawa, M. Haseyama, "POCS-based texture reconstruction method using clustering scheme by kernel PCA," *IEICE Trans. Fundamentals*, vol. E90-A, no. 8, pp. 1519–1527, Aug. 2007.

[5] J. Mairal, M. Elad, and G. Sapiro, "Sparse representation for color image restoration," *IEEE Trans. on Image Processing*, vol.17, no.1, 2008.

[6] I. Drori, D. Cohen-Or, and H. Teshurun, "Fragment-based image completion," *in SIGGRAPH 2003: ACM SIGGRAPH 2003 Papers.* New York, USA: ACM Press, pp. 303–312, 2003.

[7] A. Criminisi, P. Perez, and K. Toyama, "Region filling and object removal by exemplar-based image inpainting," *IEEE Trans. on Image Processing*, vol. 13, no. 9, pp. 1200–1212, 2004.

[8] T. H. Kwok, H. Sheung, and C. C. L. Wang, "Fast query for exemplar-based image completion," *IEEE Transactions on Image Processing*, vol. 19, no. 12, 2010.

[9] Z. Xu and J. Sun, "Image Inpainting by Patch Propagation Using Patch Sparsity," *IEEE Transactions on Image Processing*, vol. 19, no. 5, 2010.

[10] I. B. Fidaner, "A survey on variational image inpainting, texture synthesis and image completion," Available online: http://www.scribd.com/doc/3012627/A-Survey-on-Variational-Image-Inpainting-Texture-Synthesis-and-Image-Completion

[11] F. R. Fienup, "Phase retrieval algorithms: a comparison," *appl. Opt.*, vol.21, pp.2758–2769, 1982.

[12] J. C. Gower, "Adding a point to vector diagrams in multivariate analysis," *Biometrika*, vol. 55, pp.582–585, 1968.

[13] Z. Wang, A.C. Bovik, H.R. Sheikh, and E.P. Simoncelli, "Image quality assessment: From error visibility to structural similarity," *IEEE Transactions on Image Processing*, vol. 13, no. 4, pp. 600–612, Apr. 2004.

[14] T. H. Kwok and C. C. L. Wang, "Interactive image inpainting using DCT based exemplar matching," *Advances in Visual Computing, Lecture Notes in Computer Science*, vol. 5876/2009, pp.709–718, 2009.

[15] M. Bertalmio, L. Vese, G. Sapiro, and S. Ssher, "Simultaneous structure and texture image inpainting," *IEEE Trans. on Image Processing*, vol. 12, no. 8, pp. 882–889, 2003.

[16] S. D. Rane, G. Sapiro, M. Bertalmio, "Structure and texture filling-in of missing image blocks in wireless transmission and compression applications," *IEEE Trans. on Image Processing*, vol. 12, no. 3, pp. 296–303, 2003.

[17] K. Sangeetha, P. Sengottuvelan, E. Balamurugan, "Combined structure and texture image inpainting algorithm for natural scene image completion," *Journal of Information Enginerring and Applications*, vol. 1, no. 1, pp. 7–12, 2011.